

## Research papers

# Climate variability and vadose zone controls on damping of transient recharge



Claudia R. Corona <sup>a</sup>, Jason J. Gurdak <sup>a,\*</sup>, Jesse E. Dickinson <sup>b</sup>, T.P.A. Ferré <sup>c</sup>, Edwin P. Maurer <sup>d</sup>

<sup>a</sup>San Francisco State University, Dept. of Earth & Climate Sciences, San Francisco, CA, USA

<sup>b</sup>U.S. Geological Survey, Arizona Water Science Center, Tucson, AZ, USA

<sup>c</sup>University of Arizona, Dept. of Hydrology and Water Resources, Tucson, AZ, USA

<sup>d</sup>Santa Clara University, Dept. of Civil Engineering, Santa Clara, CA, USA

## ARTICLE INFO

## Article history:

Available online 30 August 2017

This manuscript was handled by Corrado Corradini, Editor-in-Chief, with the assistance of Brian D. Smerdon, Associate Editor

## Keywords:

Recharge

Climate variability

Vadose zone

Damping

Linear superposition

## ABSTRACT

Increasing demand on groundwater resources motivates understanding of the controls on recharge dynamics so model predictions under current and future climate may improve. Here we address questions about the nonlinear behavior of flux variability in the vadose zone that may explain previously reported teleconnections between global-scale climate variability and fluctuations in groundwater levels. We use hundreds of HYDRUS-1D simulations in a sensitivity analysis approach to evaluate the damping depth of transient recharge over a range of periodic boundary conditions and vadose zone geometries and hydraulic parameters that are representative of aquifer systems of the conterminous United States (U.S.). Although the models were parameterized based on U.S. aquifers, findings from this study are applicable elsewhere that have mean recharge rates between 3.65 and 730 mm yr<sup>-1</sup>. We find that mean infiltration flux, period of time varying infiltration, and hydraulic conductivity are statistically significant predictors of damping depth. The resulting framework explains why some periodic infiltration fluxes associated with climate variability dampen with depth in the vadose zone, resulting in steady-state recharge, while other periodic surface fluxes do not dampen with depth, resulting in transient recharge. We find that transient recharge in response to the climate variability patterns could be detected at the depths of water levels in most U.S. aquifers. Our findings indicate that the damping behavior of transient infiltration fluxes is linear across soil layers for a range of texture combinations. The implications are that relatively simple, homogeneous models of the vadose zone may provide reasonable estimates of the damping depth of climate-varying transient recharge in some complex, layered vadose zone profiles.

© 2017 Elsevier B.V. All rights reserved.

## 1. Introduction

A growing number of studies report that groundwater levels can fluctuate in response to low frequency and persistent global-scale climate patterns that have quasi-periodic oscillations on interannual to multidecadal timescales (e.g., Fleming and Quilty, 2006; Holman et al., 2009; Perez-Valdivia et al., 2012; Tremblay et al., 2011; Venencio and García, 2011), which affect infiltration and recharge. Complicating the interpretation of these teleconnections is that groundwater levels also respond to groundwater pumping trends and variability largely on seasonal timescales (Gurdak, 2017). This so-called *climate-induced pumping* has been detected on timescales ranging from less than one year (Russo and Lall, 2017) to scales consistent with the El Niño/Southern

Oscillation (ENSO) (Gurdak et al., 2007). These physical mechanisms have largely been inferred from statistical and spectral analysis of hydroclimatic time series (e.g., Gurdak et al., 2007; Hanson et al., 2006, 2004; Holman et al., 2011; Kuss and Gurdak, 2014; Russo and Lall, 2017). However, teleconnections that have not been evaluated by mechanistic models may be limited for understanding and predicting groundwater responses to future climate.

Increasing demands on groundwater resources from the Water-Energy-Food Nexus (Taniguchi et al., 2017) and climate variability and change (Green et al., 2011; Taylor et al., 2012) continues to raise the importance of understanding and accurately predicting current and future recharge (Meixner et al., 2016). These predictions can be improved through a better understanding of the properties of the vadose zone that control a time-varying recharge response to climate variability (Hunt et al., 2008). Such controls are poorly understood because of the nonlinear relations among unsaturated flow, pressure, water content, and hydraulic diffusivity in

\* Corresponding author.

E-mail address: [jgurdak@sfsu.edu](mailto:jgurdak@sfsu.edu) (J.J. Gurdak).

the vadose zone (Dickinson et al., 2014). These challenges are further compounded by a general lack of long-term field observations of such variables from the vadose zone that are necessary to detect time-varying recharge in response to climate variability on inter-annual to multidecadal timescales (Gurdak et al., 2007); although recent studies have begun monitoring the vadose zone under different climate regimes and land use (e.g., Baram et al., 2012; Carrera-Hernandez et al., 2011; Strobach et al., 2014; Turkeltaub et al., 2014).

As noted by Dickinson et al. (2014), the nonlinear complexity of controls on transient recharge has often limited the direct representation of recharge in groundwater models and resource assessments, which in many cases have assumed a long-term, steady-state recharge flux. Under some conditions, assigning a slowly varying or constant recharge flux in a groundwater model is justified because periodic or episodic variations in surface infiltration fluxes smooth out or dampens with depth prior to recharge (Dickinson et al., 2014). However, recent physically-based modeling studies (Dickinson et al., 2014; Velasco et al., 2015) and the previously mentioned studies that use time-series and spectral analysis have identified some conditions where climate variability results in transient recharge fluxes that are not dampened within the vadose zone. An improved ability to model recharge is relevant for improving prediction of groundwater response to future climate and the associated global-to-local scale management decisions and policy regarding sustainable groundwater (Famiglietti, 2014). This is particularly needed for aquifers in semi-arid and arid climates that often are in overdraft conditions, have relatively thick vadose zones, and are generally predicted to have less recharge and (or) more episodic recharge events under future climate change (Green et al., 2011; Taylor et al., 2012; Treidel et al., 2012). To address this need requires a review of the state of understanding of coupled climate variability and vadose zone dynamics.

### 1.1. Climate variability

The expected trends in many hydrologic processes, including recharge rates and mechanisms due to human-induced climate change, particularly over the first-half of the 21st century, can only be fully appreciated when combined with understanding of the overprinted global-scale climate variability. The majority of climate change impact studies on recharge have largely focused on human-induced climate change, often using the approach of coupling downscaled climate data from global circulation models (GCMs) that drive hydrologic models to estimate recharge rates and mechanisms under future climate change, commonly by the middle to end of the 21st century (Green et al., 2011; Meixner et al., 2016; Taylor et al., 2012; Treidel et al., 2012). The current generation of GCMs project that mean climate across many regions of the globe will move to a state continuously beyond historical variability by the mid-21st century (Mora et al., 2013), which will likely alter the frequency, magnitude, and other spatiotemporal characteristics of climate variability patterns (Stoner et al., 2009). However, the comparatively short-term planning horizon (often years to decades) for most groundwater resource management decisions means that transient recharge in response to climate variability on interannual to multidecadal timescales has immediate and tangible implications for groundwater sustainability (Gurdak et al., 2009).

Climate variability occurs on all temporal scales that extend beyond weather events, and is defined as the difference between current climate conditions and the mean state over a larger temporal scale (Ghil, 2002). Climate variability is often characterized using indices that combine sea surface temperatures, sea level pressures, geo-potential heights, and wind speed, among other atmosphere–ocean variables (Ghil, 2002). The indices that represent

the six leading atmospheric–ocean circulation systems that affect North American interannual to multidecadal climate variability include the Atlantic teleconnection patterns: the Arctic Oscillation (AO), North Atlantic Oscillation (NAO), and Atlantic Multidecadal Oscillation (AMO); and the Pacific teleconnection patterns: ENSO, Pacific Decadal Oscillation (PDO), and Pacific–North American Oscillation (PNA). The most widely accepted quasi-periodic cycles for these systems range from <1–70 years, including 6–12 months (AO), 3–6 years (NAO), 50–70 years (AMO), 2–7 years (ENSO), 15–30 years (PDO), to <1–4 years (PNA) (Enfield et al., 2001; Ghil, 2002; Hurrell, 1995; Kuss and Gurdak, 2014; Mantua and Hare, 2002; NOAA, 2015; Stoner et al., 2009; Wolter and Timlin, 2011). While GCMs vary in their ability to represent these cycles skillfully, recent analysis demonstrate some robust projections for how they may evolve through the 21st century, such as changing in amplitude, time scale, and increasing the meteorological extremes with which they are associated (Chen et al., 2017; Zhang and Delworth, 2016).

The Atlantic and Pacific teleconnections influence the spatiotemporal patterns of precipitation, air temperature, drought, snowpack and melt, evapotranspiration, stream discharge, and other land-surface hydrologic processes across the continental U. S, North America, and other regions (Bayari and Yildiz, 2012; Beebe and Manga, 2004; Brabets and Walvoord, 2009; Cayan et al., 1999; Enfield et al., 2001; Kondrashov et al., 2005; Maheu et al., 2003; Mantua et al., 1997; Mazouz et al., 2012; McCabe et al., 2004; Ropelewski and Halpert, 1986; Sabziparvar et al., 2011; Tremblay et al., 2011; Vicente-Serrano et al., 2011). Such variability in surface hydroclimatology is expected to influence time-varying infiltration, downward water flux in the vadose zone, and ultimately recharge rates and mechanism (Gurdak et al., 2007; Hanson et al., 2004; Kuss and Gurdak, 2014). However, the teleconnections patterns that exist in surface hydrologic processes are not necessarily the same as those preserved in the subsurface processes that affect groundwater levels (Velasco et al., 2015). Much of the subsurface hydrologic response is also a function of the hydraulic properties of the vadose zone (Dickinson et al., 2014).

### 1.2. Vadose zone hydraulic properties and climate-varying recharge

Recent research has begun to consider the properties of the vadose zone that may influence whether groundwater levels may respond to climate variability. To investigate the role of the vadose zone, these studies have focused on the relations between soil and water properties and periodic flow in the vadose zone that could be driven by climate variability (Bakker and Nieber, 2009; Dickinson et al., 2004, 2014; Pool and Dickinson, 2007). These relations become important when climatic forcings at the land surface can be damped in the vadose zone prior to reaching the water table (Velasco et al., 2015). Bakker and Nieber (2009) derived an analytical solution to the Richards equation for vertical, one-dimensional transient flow that was used to predict the movement of cyclical, sinusoidally-varying fluxes at the land surface where the infiltration can be assumed to be a function of precipitation and evaporation. Bakker and Nieber (2009) found that flux variations damp with depth in the vadose zone such that beyond a certain depth (referred as the damping depth ( $d$ )), the flux could be approximated as steady (Bakker and Nieber, 2009).

Expanding on the work of Bakker and Nieber (2009), Dickinson et al. (2014) developed a screening tool for evaluating how variability of a cyclical infiltration pattern at the land surface was damped with depth in the vadose zone. If the flow variability damped to within 5% of the original amplitude, they stated that the assigned recharge in numerical groundwater flow models can be assumed to be steady. However, if >5% of the infiltration variability remained at the depth of the water table, recharge is

assumed to be transient. Dickinson et al. (2014) assessed the sensitivity of the damping to vertical water fluxes typical of arid and semiarid regions where the periods of infiltration variability ranged from 1 to 365 days in homogenous sand and clay. The damping and damping depth was evaluated through comparisons with results from numerical simulations from the software HYDRUS-1D (Šimůnek et al., 2008). Dickinson et al. (2014) found that the analytical solution by Bakker and Nieber (2009) was most accurate for soil–water conditions where the hydraulic diffusivity is relatively constant. The hydraulic diffusivity is likely to be steady in fine soils when both the water content and flux variability are relatively small. They found that the diffusivity can be highly variable in coarse soils, such as sand when the amplitude of the flux variability and water content were relatively large. Dickinson et al. (2014) found that the damping depth from the analytical solution (Bakker and Nieber, 2009) could be excessively large, up to five times the damping depth from the numerical solution, when the diffusivity was highly variable. This overestimation of the numerical damping depth, which is also an underestimation of the damping, may result in mischaracterization of the damping properties of the vadose zone. In their examples, Dickinson et al. (2014) noted that regions of coarse soils in aquifers where recharge was likely to be steady could have been misidentified as having transient recharge. Their analysis was limited to homogeneous sand and clay soils, and damping in layered soils with contrasting soil–water properties was not assessed.

### 1.3. Objectives

This paper addresses the knowledge gap of how physical processes of water flow in the vadose zone contribute to observed teleconnections between climate and groundwater levels by controlling transient recharge fluxes and mechanisms in response to climate variability. Here we systematically build on the findings of Dickinson et al., (2014) by using a sensitivity analysis approach to evaluate the damping of cyclical surface forcings in the vadose zone from hundreds of numerical HYDRUS-1D simulations over a range of periodic boundary conditions and vadose zone geometries and hydraulic parameters that are generally representative of aquifer systems of the conterminous United States (U.S). We assess the damping properties of the vadose zone using a numerical approach that allows for a more accurate, time-varying hydraulic diffusivity than the approach by Dickinson et al. (2014). We use the results of this approach to address the following research questions: How does soil texture in the vadose zone influence damping in homogeneous (one layer) and heterogeneous (two layer) systems? What

are the effects of layer thickness on damping depth ( $d$ )? Does the damping in two layers occur independently, or does the presence of one layer impact the damping in the other layer? If the damping is independent, is linear superposition (described in Section 2.1.4) of the damping in separate layers a reasonable approximation? Which characteristics of the infiltration and soil–water parameters have the most statistically significant influence on  $d$ ? By addressing these questions surrounding  $d$ , we provide a framework that can be used to (i) interpret the physical processes underlying the teleconnections between climate variability patterns and fluctuations in groundwater levels and (ii) predict steady-state versus transient recharge over a wide range of time-varying infiltration fluxes, periods, and hydraulic properties of soil and vadose zone that is representative of U.S. aquifers.

## 2. Methods

### 2.1. Numerical modeling

Numerical HYDRUS-1D (Šimůnek et al., 2008) simulations were used to evaluate the hydraulic properties and characteristics of the periodic net infiltration flux ( $q_z$ ) affecting the  $d$  and transient recharge in homogeneous (one layer) and heterogeneous (two layer) textural profiles of the vadose zone. HYDRUS-1D is a computer program that solves the Richards equation for saturated and unsaturated water flow. In general, two sets of HYDRUS-1D simulations were run; one for homogeneous (one layer) profiles and one for heterogeneous (two layer) profiles. This section describes the model conditions and parameters that were used in both sets of HYDRUS-1D simulations (Table 1), while the details about the homogeneous and heterogeneous simulations are described in the subsequent sections.

The boundary conditions to the HYDRUS-1D simulations were a periodic vertical, net infiltration flux ( $q_{z=0}$ ) [ $L T^{-1}$ ] below the root zone at depth  $z = 0$  and free drainage and the gradient of total head is equal to 1. The flux  $q_{z=0}$  is a composite of a steady, downward mean flux ( $q_s$ ) [ $L T^{-1}$ ] and a sinusoidal transient component with mean amplitude ( $q_p$ ) [ $L T^{-1}$ ] value and period,  $P$  [T] (Fig. 1a). The combined  $q_s$  and  $q_p$  components represents the net infiltration below the root zone that results from the infiltration of precipitation, runoff, and the uptake of water by evapotranspiration. The components of  $q_z$  can represent varying infiltration in diffuse recharge settings, basin floors, stream channels, or areas of applied irrigation water, where the steady component,  $q_s$ , represents a long-term mean flux and the periodic component,  $q_p$ , represents the sum of episodic events and climate variations from the steady

**Table 1**

Overview of model conditions and parameters used in the HYDRUS-1D (Šimůnek et al., 2008) simulations of homogeneous and heterogeneous profiles of the vadose zone. Note – the number (#) of soil textures is listed in Table 4.

Condition or parameter	Homogeneous (one layer) profile	Heterogeneous (two layer) profile
Geometric parameter: Depth of profile, m	10, 20, 100 m	10 and 50 m
Initial conditions: – Mean water flux, $q_s$ ; – Amplitude of the sinusoidal flux, $q_p$ ; – Period, $P$	All (see Tables 2 and 3); All (see Tables 2 and 3); 30, 90, 180, 365 days and 2, 7, 10 years	1.0 mm d <sup>-1</sup> ; 0.99 mm d <sup>-1</sup> ; 30, 90, and 365 days
Soil texture: hydraulic properties and Gardner hydraulic parameters.	#1–12 (see Table 4)	Soil texture of upper over lower layer: #1 over 5 and 7; #5 over 1 and 7; #7 over 1 and 5;
Boundary conditions: – Upper boundary condition – Lower boundary condition	Constant flux Free drainage	Constant flux Free drainage

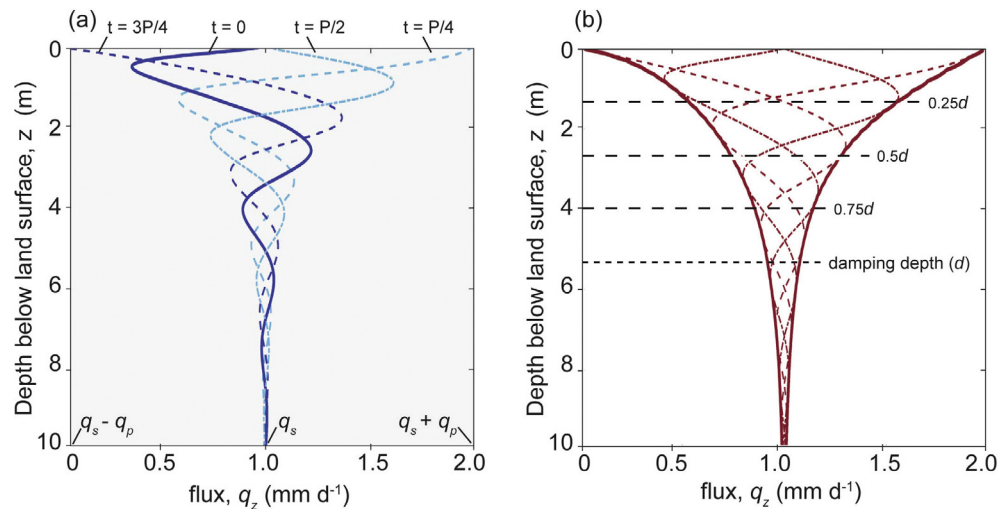


**Fig. 1.** (a) Damping of a sinusoidal vertical flux,  $q_z$  [ $L T^{-1}$ ], applied at land surface, where  $z = 0$ . Profiles of the flux with depth at times  $0, P/4, P/2$ , and  $3P/4$ , where  $P$  [T] is the sinusoidal wave period. The flux travels vertically downward and has a steady component,  $q_s$ , plus a sinusoidal component with amplitude  $q_p$ . Modified from Dickinson et al. (2014). (b) The  $q_z$  damps to some depth ( $z$ ), where the damping depth ( $d$ ) is equal to  $\delta = 0.05$ . For the heterogeneous (two layer) HYDRUS-1 D simulations, the upper layer thickness is defined in the model domain as a function of  $d$ , where relatively thin upper layer is  $0.25d$ , intermediate thickness upper layer is  $0.5d$ , and relative thick upper layer is  $0.75d$ .

**Table 2**

Calculated net infiltration rates used to specify the downward mean flux,  $q_s$  [ $P$ , mean annual precipitation; and  $ET$ , mean annual evapotranspiration used from Sanford and Selnick (2013)].

Regions	ET/P ratio	Infiltration Rate	Climate
Arid Southwest	>80%	0.01–0.10 $mm d^{-1}$	Little to no rainfall, high temperatures
Temperate	70–50%	0.50 $mm d^{-1}$	Moderate rainfall, moderate temperatures
WEST: Cascade Mts, Sierra Mts, Northern Rocky Mts, EAST: New England, Appalachian Mountains, Central Gulf Coast	50–30%	1.00 $mm d^{-1}$	Moderate temperatures, high rainfall
Pacific Northwest	<20%	2.00 $mm d^{-1}$	High rainfall, low-to-moderate temperatures

component. For a real system where distributed recharge is characterized, the sum of  $q_s$  at all locations would equal the total discharge. For our analysis, the amplitude  $q_p$  never exceeds the steady component of the flux,  $q_s$  (Bakker and Nieber, 2009; Dickinson et al., 2014). This results in a flux that is always positive in the downward direction.

The  $q_s$  values were selected to represent long-term (1971–2000) mean net recharge rates from a range of climate and land-cover regions of the conterminous U.S., and were calculated as the difference between mean annual precipitation and mean annual evapotranspiration, as reported by Sanford and Selnick (2013) (Table 2). This residual contains both recharge and runoff, and may overestimate recharge in some areas. Table 3 summarizes the  $q_s$  values used in the HYDRUS-1D simulations to represent different climate

**Table 3**

Downward mean flux ( $q_s$ ) and mean amplitude ( $q_p$ ) values using in the HYDRUS-1D simulations.

Climate and Land Cover Region	Mean Flux, $q_s$ ( $mm d^{-1}$ )	Mean Amplitude, $q_p$ ( $mm d^{-1}$ )	Mean Annual Flux ( $mm yr^{-1}$ )
Arid	0.01	0.00990	3.65
	0.025	0.02475	9.13
Semi-arid	0.05	0.0495	18.3
	0.10	0.099	36.5
Shrub-land	0.50	0.495	183
Grassland	1.00	0.99	365
Forest, Marsh	2.00	1.98	730

and land cover regions. Although the models were parameterized based on U.S. aquifers and climate, findings from this study are applicable elsewhere that have mean recharge rates between 3.65 and 730  $mm yr^{-1}$  (Table 3). The amplitude of the sinusoidal flux component  $q_p$  were set equal to 99% of each  $q_s$ , thus the flux is always downward and greater than zero (Table 3).

A range of periods ( $P$ ) were used in the HYDRUS-1D simulations to represent  $q_{z=0}$  variability on monthly (30 day), seasonal (90 and 180 day), and annual (365 day) timescales (Table 1). The 30 day periods are used to represent synoptic-scale meteorological systems, while the 90 and 180 day periods represent Mediterranean, monsoonal, or other climates that have distinct wet and dry seasons. In addition, longer periods of 730, 2,556, and 3,652 days (2, 7, and 10 years, Table 1) were used in the simulations to represent  $q_{z=0}$  variability that is consistent with global-scale climate patterns, including PNA (<1–4 years), NAO (3–6 years), and ENSO (2–7 year) cycles. The Hydrus-1D models were spun up for at least 20 periods to achieve oscillatory steady-state conditions prior to evaluating the transient responses.

The HYDRUS-1D soil texture and hydraulic properties were parameterized using the 12 U.S. Department of Agriculture (USDA) soil textural classes and the Gardner (1958) and Gardner-Kozeny (Mathias and Butler, 2006; Bakker and Nieber, 2009) soil hydraulic models, except for the saturated hydraulic conductivity ( $K_s$ ) values that were obtained from the Rosetta soil catalog (Schaap et al., 2001) (Table 4). The Gardner  $\alpha$  and Gardner-Kozeny  $n_0$  and  $\mu$  parameter values (Table 4) were estimated by linear regression as detailed in Dickinson et al. (2014) and Wraith and Or (1998).

**Table 4**  
U.S. Department of Agriculture (USDA) soil textural classes and Gardner hydraulic parameters used in the HYDRUS-1D simulations (modified from Dickinson et al., 2014).

#	Soil Texture	$K_{\text{sat}}$ ( $\text{m d}^{-1}$ )	$\alpha$ ( $\text{m}^{-1}$ )	$\psi_e$ (m)	$n_0$	$\mu$	$\theta_{\text{residual}}$ ( $\text{m}^3 \text{m}^{-3}$ )	$\theta_{\text{saturated}}$ ( $\text{m}^3 \text{m}^{-3}$ )
1	clay	0.15	6.87	-0.366	0.459	2.046	0.098	0.459
2	silty clay	0.09	7.34	-0.334	0.481	2.184	0.111	0.481
3	silty clay loam	0.11	4.43	-0.695	0.482	1.323	0.090	0.482
4	silt loam	0.18	3.20	-1.189	0.439	0.956	0.065	0.439
5	silt	0.44	3.76	-0.902	0.489	1.123	0.050	0.489
6	clay loam	0.08	7.19	-0.344	0.442	2.139	0.079	0.442
7	loam	0.12	5.44	-0.511	0.399	1.623	0.063	0.489
8	sandy clay	0.11	13.7	-0.134	0.385	4.076	0.061	0.385
9	sandy clay loam	0.13	9.14	-0.244	0.384	2.719	0.063	0.384
10	sandy loam	0.38	11.2	-0.182	0.387	3.334	0.039	0.387
11	loamy sand	1.05	14.2	-0.127	0.390	4.223	0.049	0.390
12	sand	6.43	14.4	-0.124	0.375	4.276	0.053	0.375

### 2.1.1. Homogeneous (one layer) profiles

A total of 588 HYDRUS-1D simulations of homogeneous (one layer) profiles were run for all combinations of the 12 USDA soil textures (Table 4), seven mean fluxes ( $q_s$ ) (Table 3), and seven periods (P) (Table 1). The model domain includes 1001 nodes with a vertical node spacing that is equal and sums to the specified bottom boundary of the model, which included 10, 20, and 100 m (Table 1). The larger profile (bottom boundary) depths of 20 and 100 m were used in simulations where the  $d$  exceeded the 10 m profile depth. The results of the homogeneous profile simulations were used as a guide to constrain the range of model conditions and parameters tested during the subsequent HYDRUS-1D simulations of heterogeneous (two layer) profiles.

### 2.1.2. Heterogeneous (two layer) profiles

A total of 54 HYDRUS-1D simulations of heterogeneous (two layer) profiles were run for all layer combinations of three representative USDA soil textures (clay, silt, and loam; Table 1), one mean flux ( $q_s$ ) ( $1.00 \text{ mm d}^{-1}$ ; Table 1), three periods (P) (30, 90, and 365 days; Table 1), and three relative thicknesses (thin, intermediate, and thick) of the upper layer in the two-layered profile. Similar to the homogeneous simulations, the model domain for the two-layered profile included 1001 nodes with equal vertical node spacing over depths from 10 m and 50 m (Table 1). Here we evaluate two layers to keep the problem tractable to better understand the behavior between layers. The larger profile depth (bottom boundary) of 50 m was used in simulations where the  $d$  exceeded the 10 m profile depth.

Here we establish the relative thickness (thin, intermediate, and thick) of the upper layer using quarter fractions of the  $d$  that resulted from the HYDRUS-1D simulations of the homogeneous (one layer) profiles (Fig. 1b). Using this approach, a relatively thin upper layer is  $0.25d$ , intermediate thick upper layer is  $0.5d$ , and relatively thick upper layer is  $0.75d$  (Fig. 1b). This creates a set of three possible upper layer thicknesses for each of the two-layered model domains (Table 1). Once the thickness of the upper layer is established, the remaining lower portion of the model domain is set as the lower layer. Therefore, the thickness of the lower layer is a function of the upper-layer thickness.

### 2.1.3. Vertically stacked homogeneous profiles

The simulated damping depth from vertically stacked homogeneous profiles of flux variability (Fig. 2), which is used to approximate the flux variability in two layers in a single simulation and help test for linearity and superposition (see Section 2.1.4), is calculated as follows. First, flow in the upper layer was simulated by HYDRUS-1D with a single homogeneous soil layer to represent the damping in an upper soil layer (Fig. 2c). Next, the  $q_p$  from the bottom of the upper layer defines the input  $q_p$  for the simulation

of flow in a single homogeneous, lower layer to represent a lower layer (Fig. 2c and d). The simulation of the homogeneous, upper layer is similar to the description from Section 2.1 in that the mean amplitude of the sinusoidal flux component  $q_p$  (at  $z=0$ ) was set equal to 99% of the  $q_s$  (Fig. 2c). However, the separate simulation of the homogeneous, lower layer (Fig. 2d) uses as input (at  $z=0$ ) the  $q_p$  from the bottom of the homogeneous, upper layer, rather than being set equal to 99% of the  $q_s$ . Finally, the damping depth of the vertically stacked homogeneous profiles ( $d_{\text{shp}}$ ) (Fig. 2c and d) is calculated as:

$$d_{\text{shp}} = z_{\text{ul}} + d_{\text{ll}} \quad (1)$$

where  $z_{\text{ul}}$  [L] is the relative thickness (thin,  $0.25d$ ; intermediate,  $0.5d$ ; or thick,  $0.75d$ ) used in the simulation of the homogeneous, upper layer, and  $d_{\text{ll}}$  [L] is the damping depth simulated in the lower layer.

### 2.1.4. Testing for linearity and superposition

We explore the approximation of linear superposition with respect to the damping depth ( $d$ ) and the interactions between layered soil textures in the vadose zone. If the assumption of linear superposition holds true, we expect that adding the  $d$  from simulations of two separate homogeneous soil profiles should approximate the simulated  $d$  in a layered system of the same two soil textures. The implications of linear superposition would enable using  $d$  behavior in homogeneous soil profiles to estimate  $d$  behavior, and hence steady-state and transient recharge in more complex layered soil profiles that are representative of natural vadose zones.

To test the linear superposition approximation, we first simulate damping depths in heterogeneous (two layer) soil profiles ( $d_{2\text{lp}}$ ) when the upper layer has different relative thicknesses (thin, intermediate, and thick) (Fig. 2b). That is, we simulate flow in two layers in a single HYDRUS-1D model. Then, we compare the  $d_{2\text{lp}}$  to the simulated damping depths from vertically stacked homogeneous profiles ( $d_{\text{shp}}$ ) (Fig. 2c and d). We consider the linear superposition approximation to be reasonably accurate if:

$$d_{\text{shp}}(\pm 10\%) = d_{2\text{lp}} \quad (2)$$

where the damping depth from vertically stacked homogeneous profiles ( $d_{\text{shp}}$ ) is within  $\pm 10\%$  of the simulated damping depths in the heterogeneous (two layer) profiles ( $d_{2\text{lp}}$ ). Fig. 2 illustrates an example where the  $d_{\text{shp}}$  is 13.7% greater than the  $d_{2\text{lp}}$  and linear superposition may not be valid. However, the cases where Eq. (2) are true indicate that  $d$  is largely influenced by the hydraulic properties of the upper layer, with relatively smaller influence by the hydraulic interactions between the layers or properties of the lower layer. An important implication of the linear superposition assumption

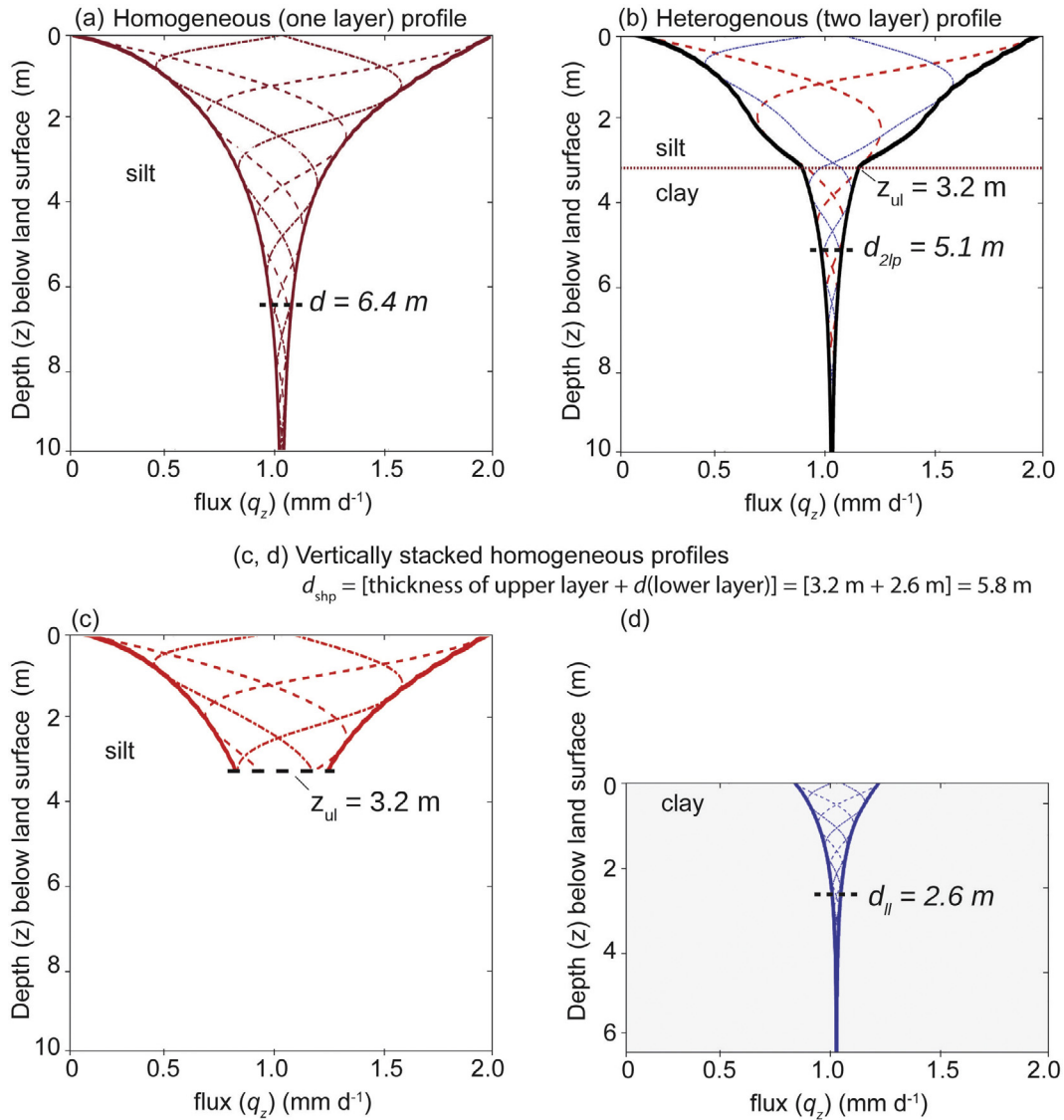


**Fig. 2.** Example calculation of damping depths from vertically stacked homogeneous profiles ( $d_{shp}$ ) using the HYDRUS-1D simulations. For comparison, the vertical flux,  $q_z = 1.0 \text{ mm d}^{-1}$ , with Period ( $P$ ) = 90 days applied at land surface ( $z = 0$ ) damps to different damping depths ( $d$ ) in HYDRUS-1D simulations of (a) homogeneous (one layer) profile of silt ( $d = 6.4 \text{ m}$ ), (b) heterogeneous (two layer) profile of intermediate (0.5d) thickness ( $z_{ui} = 3.2 \text{ m}$ ) silt layer over clay layer ( $d_{2lp} = 5.1 \text{ m}$ ), and (c, d) vertically stacked homogeneous profiles ( $d_{shp} = 5.8 \text{ m}$ ). The  $d_{shp}$  is calculated as the sum of the (c) upper layer thickness ( $z_{ui} = 3.2 \text{ m}$ ) and (d) damping depth in lower layer ( $d_{1l} = 2.6 \text{ m}$ ). Note that in (c), the simulated flux variability continues at depths greater than  $z_{ui} = 3.2 \text{ m}$ , which we have not shown here for illustration purposes. The (c) simulated  $q_p$  from the  $z_{ui}$  of the homogeneous, silt simulation is used as the (d) input  $q_p$  ( $z = 0$ ) for the simulation of the homogeneous, clay simulation. In this example, the  $d_{shp}$  (5.8 m) is 13.7% greater than the  $d_{2lp}$  (5.1 m).

tion is that simple, homogeneous models may provide reasonable estimates of  $d$  in more complex, layered systems.

### 2.2. Significance testing

We used the False Discovery Rate (FDR) technique (Benjamini and Hochberg, 1995) during the statistical significance testing to quantify the relative sensitivity of  $d$  to  $K$ ,  $q_s$ , and  $P$ . The FDR p-value adjustment efficiently controls for the rate of false positives among a large number of tests (Benjamini and Hochberg, 1995). The FDR p-values ( $p_{(i), FDR}$ ) are computed as:

$$p_{(i), FDR} = \text{Minimum} [p(i + 1, FDR), (m/i)p(i)] \quad (3)$$

where the independently calculated p-values have an FDR adjusted p-value that falls below  $\alpha$  if the parameter is statistically significant at the 0.05 level (Benjamini and Hochberg, 1995). We used the FDR

LogWorth transformation (Benjamini and Hochberg, 1995) to provide an appropriate scale for visualization, where:

$$-\log_{10}(\text{FDR } p\text{-value}) = 1.3 \quad (4)$$

$$-\log_{10}(0.05) = 1.3$$

A FDR LogWorth value  $>1.3$  indicates significance at the 0.05 level. We use the FDR LogWorth approach to reject the null hypothesis that the  $K$ ,  $q_s$ , and  $P$  do not influence  $d$ . We also present the  $R^2$  values from the linear least squares model to evaluate the proportion of variation in  $d$  that is accounted for by the  $K$ ,  $q_s$ , and  $P$ .

### 3. Results and discussion

The results and discussion are organized in two parts to address the research questions. First, we present results from the simula-

tions of the homogenous (one layer) profiles and discuss how  $d$  is influenced by the hydraulic properties of the vadose zone and characteristics of the net infiltration flux,  $q_s$ . Second, we present results from the simulations of the heterogeneous (two layer) profiles and vertically stacked homogeneous profiles, and discuss how  $d$  is influenced by layer thickness, layer interactions, and the conditions where the assumption of linear superposition is valid.

3.1. Damping depth in homogenous (one layer) profiles ( $d$ )

Results from the simulations of homogeneous (one layer) profiles indicate that  $d$  is positively related to  $q_s$  and  $P$ . To illustrate this relation, we show the simulated  $d$  for three representative soil textures (clay, silt, and loam) and ranges of  $q_s$  (0.01–1.0 mm d<sup>-1</sup>) and  $P$  (30–730 days) (Fig. 3). The  $d$  associated with arid  $q_s$

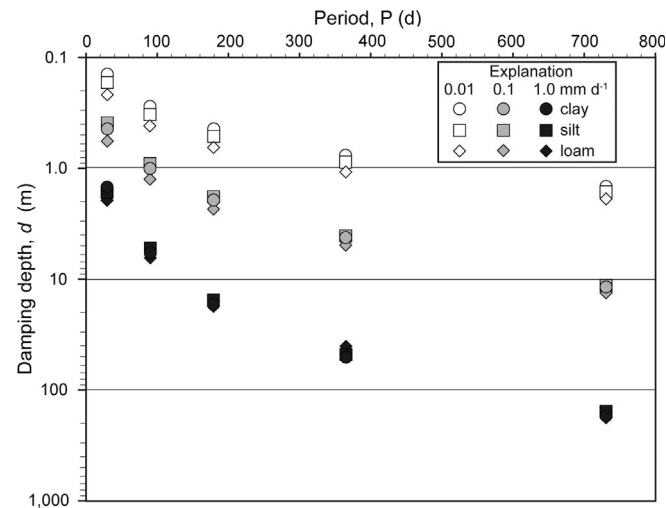


Fig. 3. Comparison of damping depths,  $d$  (m) resulting from HYDRUS-1D simulation of homogeneous (one layer) profiles of a representative range of three soil textures (clay, silt, and loam), three mean fluxes,  $q_s$  (0.01, 0.1, and 1.0 mm d<sup>-1</sup>), and five periods,  $P$  (30, 90, 180, 365, and 731 days).

(0.01 mm d<sup>-1</sup>) remains within the upper 2 m even with  $P$  that is consistent with ENSO variability (730 days) (Fig. 3). However, the larger  $q_s$  associated with semi-arid (0.1 mm d<sup>-1</sup>) and humid (1.0 mm d<sup>-1</sup>) climates results in  $d$  that span from <1 m under monthly and seasonal  $P$  (30–90 days) to >100 m for  $P$  that is consistent with ENSO variability (Fig. 3). The simulated  $d$  is similar in the clay, silt, and loam profiles, even as  $q_s$  and  $P$  increase (Fig. 3).

Results from all simulations of homogeneous (one layer) profiles indicate that  $d$  spans more than four orders-of-magnitude from 0.1 to >1000 m (Fig. 4). The  $d$  exceeds >1000 m in simulations using  $q_s \geq 0.05$  mm d<sup>-1</sup> and  $P \geq 2557$  d, but those results are not shown here because the thickness of the vadose zone is generally <1000 m in aquifers (Fan et al., 2007). Fig. 4 illustrates three important positive relations: the  $d$  generally increases as a function of increasing coarseness of soil texture and increasing  $q_s$  and  $P$ , which are findings that are generally consistent with Dickinson et al. (2014). The reader is referred to Corona (2016) for tables of values used in Fig. 4. As the  $q_s$  and  $P$  increase, the sensitivity of  $d$  to the differences in hydraulic properties of the soil texture also increases, particularly for the relatively coarser soil textures. The implications of these results is that vadose zone sediment with greater sand content is likely to preserve transient recharge fluxes associated with climate variability, especially those at greater  $q_s$  and  $P$ , at relatively greater depths to water than vadose zone sediments with more silt, clay, and loam, which is a finding consistent with Dickinson et al. (2014). The effect of sediment texture on  $d$  is further explored in the results from the simulations of the heterogeneous (two layer) profiles and vertically stacked homogeneous profiles.

While vertical heterogeneities in soil texture are ubiquitous in real-world vadose zones, the findings about homogeneous soil textures shown in Fig. 4 begin to illustrate some important possible implications for the detection of spatial and temporal patterns of transient recharge in response to climate variability across U.S. aquifers. The depth to water (or vadose zone thickness) is generally less than 100 m in most aquifers of the U.S. (Fan et al., 2007). Aquifers in the humid ( $q_s$ , 0.50–2.0 mm d<sup>-1</sup>), eastern U.S. tend to have relatively smaller depths to water, often less than 10–20 m, while aquifers in the semiarid and arid ( $q_s$ , 0.01–0.10 mm d<sup>-1</sup>) western

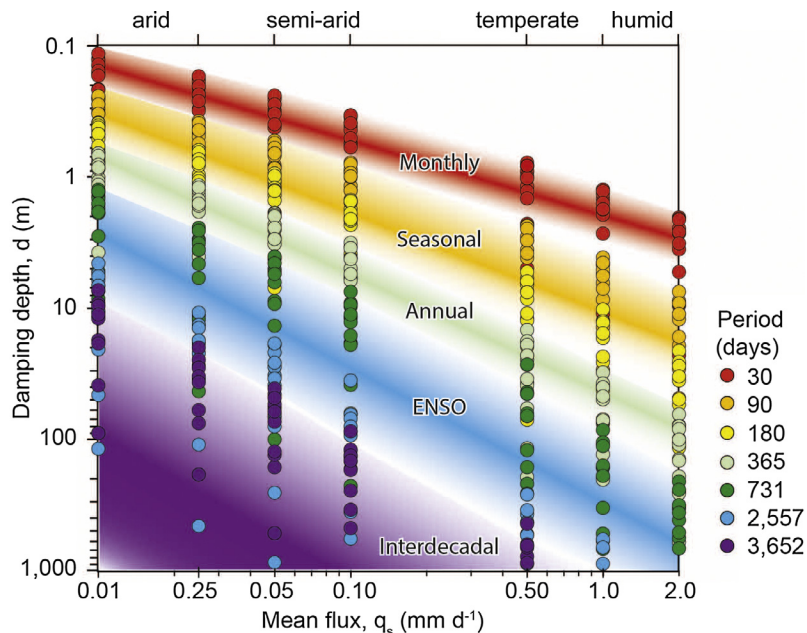


Fig. 4. Damping depths (m) resulting from 588 HYDRUS-1D simulations of homogeneous (one layer) profiles of the 12 USDA soil textures, mean fluxes ( $q_s$ ) (0.01–2.0 mm d<sup>-1</sup>), and periods ( $P$ ) (30–3652 days).

**Table 5**

The False Discovery Rate (FDR) and FDR LogWorth values from statistical significance testing and least square model.

#	Soil Texture	FDR p-values ( $\alpha = 0.05$ )			FDR LogWorth values			$R^2$
		$q_s$	P	$K_{sat}$	$q_s$	P	$K_{sat}$	
1	clay	0.0009	0.0022	0.017	3.06	2.66	1.77	0.61
2	silty clay	0.0009	0.0022	0.017	3.06	2.66	1.77	0.61
3	silty clay loam	0.0008	0.0023	0.020	3.09	2.65	1.77	0.61
4	silt loam	0.0008	0.0023	0.020	3.09	2.64	1.70	0.61
5	silt	0.0010	0.0036	0.024	3.01	2.44	1.65	0.59
6	clay loam	0.0009	0.0023	0.018	3.04	2.63	1.76	0.60
7	loam	0.0009	0.0024	0.018	3.05	2.62	1.75	0.60
8	sandy clay	0.0004	0.0015	0.014	3.38	2.82	1.87	0.63
9	sandy clay loam	0.0008	0.0022	0.016	3.56	2.84	1.80	0.61
10	sandy loam	0.0004	0.0010	0.013	3.37	3.02	1.90	0.64
11	loamy sand	0.0004	0.0005	0.013	3.46	3.32	1.90	0.66
12	sand	0.0029	0.0029	0.048	2.54	2.54	1.32	0.55

U.S. tend to have relatively greater depths to water, often 50–100 m, or more (Fan et al., 2007). Using those approximate depths to water and  $q_s$  ranges, Fig. 4 illustrates that transient recharge in response to  $q_s$  variability on seasonal (90 days) to decadal (3652 days) timescales are more likely to reach the water table in aquifers of the humid, eastern U.S., while only transient recharge with longer periods (731–3652 days) are likely to reach the water table in aquifers of the semiarid and arid U.S. The patterns of  $d$  in Fig. 4 also indicates that transient recharge with relatively shorter periods (seasonal) could be detected at the depth to water in aquifers of the semiarid and arid U.S. if focused or preferential recharge mechanisms (i.e., ephemeral streams, topographic depressions, or irrigation return flow) create local  $q_s$  rates of 0.50–2.0 mm d<sup>-1</sup>. The simulated  $d$  under the range of conditions representative of the continental U.S. (Fig. 4) shows that transient recharge in response to AO, NAO, ENSO, and possibly PDO could be detected at the depth of the water table in most aquifers, especially in those of the humid, eastern U.S.

The results of the significance testing support these interpretation of simulated  $d$  in homogeneous (one layer) profiles and indicate that  $q_s$ , P, and  $K_{sat}$  are all statistically significant ( $\alpha = 0.05$ ) variables that influence  $d$  (Table 5). In all soil textures except sand,  $d$  is the most sensitive to  $q_s$ , followed by P, and finally  $K_{sat}$ , based on the FDR LogWorth values (Table 5). In sand, the  $q_s$  and P have equal influence on  $d$ , but these results are less reliable because of numerical convergence issues in the highly nonlinear numerical simulations of flow in sand. Based on these significance tests, the variables associated with natural climate variable, such as  $q_s$  and P are relatively more important as compared to variables associated with the vadose zone, such as  $K_{sat}$  in determining the depth of transient recharge in aquifers. An implication is that prioritizing the characterization of average infiltration fluxes ( $q_s$ ) and climate variability periodicity (P) over site specific soil types, for example during groundwater model development, may yield more accurate estimates of transient versus steady recharge. These interpretations have limitations because the  $R^2$  values range from 0.55 to 0.66 (Table 5), indicating that these three variables could only explain about half to two-thirds of the variability in  $d$ . The unexplained variability in  $d$  is likely attributed to hydraulic diffusivity (D), which varies with depth and time in the vadose zone and makes such hydraulic properties difficult to evaluate with statistical significance tests.

### 3.2. Damping depth in heterogeneous (two layer) profiles ( $d_{2lp}$ )

The simulated damping depths from homogeneous (one layer) profiles ( $d$ ) are compared to damping depths from heterogeneous (two layer) profiles ( $d_{2lp}$ ) to evaluate the effects of layering and layer thickness for three representative soil textures (clay, silt,

and loam) (Fig. 5). The percent change from  $d$  to  $d_{2lp}$  ranges from –35 to 40%, and represent only comparisons between simulations where the texture from the top of the two-layer profile is the same as the texture from the one-layer profile (Fig. 5). The negative % values indicate that  $d_{2lp} < d$  in the corresponding one-layer profile, and the positive % values indicate that the  $d_{2lp} > d$  in the corresponding one-layer profile (Fig. 5). The majority of the values are between +/-25% for all three upper-layer thicknesses, and there is no observable trend in the variance of the percent change in  $d$  as a function of upper-layer thickness for most soil textures and P (Fig. 5). A few exceptions occur for the monthly P (30 days) where percent change in  $d$  is as much as 30% greater for the relatively thin upper layer compared to the relatively thick upper

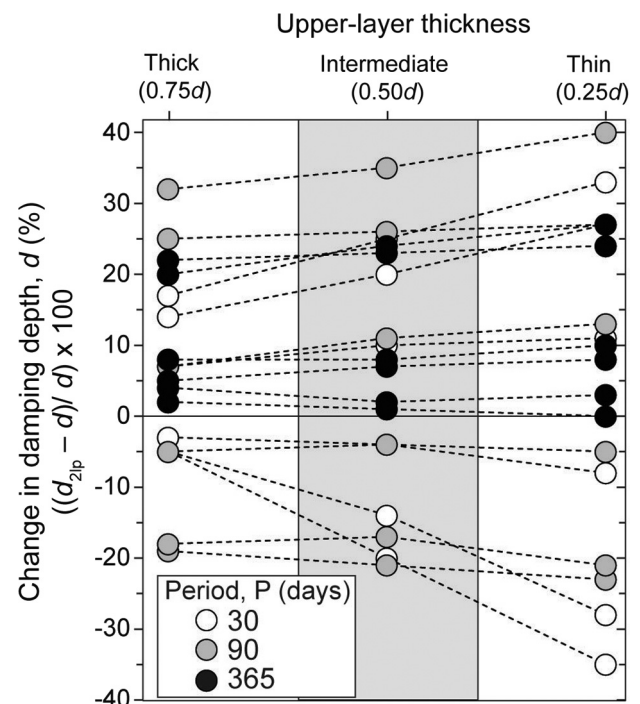


**Fig. 5.** The percent change (%) between 54 HYDRUS-1D simulations of damping depth in homogeneous (one layer) profiles ( $d$ ) and damping depth in heterogeneous (two layer) profiles ( $d_{2lp}$ ) is shown as a function of upper-layer thickness (thick, 0.75d; intermediate, 0.5d; and thin, 0.25d) for three representative soil textures (clay, silt, and loam). The percent change between  $d$  and  $d_{2lp}$  are calculated using only simulations where the texture from the homogeneous (one layer) profile is the same as the upper-layer texture from the heterogeneous (two layer) profile, using the same  $q_s$  (1.0 mm d<sup>-1</sup>) and P (30, 90, or 365 days). The negative % values indicate that  $d_{2lp} < d$  in the corresponding one-layer profile, and the positive % values indicate that the  $d_{2lp} > d$  in the corresponding one-layer profile. The dashed lines connect the same combinations of upper- and lower-layer soil textures.

(Fig. 5). However, the results indicate that  $d_{2lp}$  is generally not sensitive to the upper-layer thickness for the range of  $q_s$ , monthly to annual P, and for most soil textures. The implications are that when the soil textures in a layered profile include clay, silt, and loam, homogeneous simulations that use the soil texture representative of land surface may provide reasonable approximations ( $\pm 25\%$ ) of the depth of transient recharge as compared to more complex heterogeneous simulations that parameterize layering of texture in the vadose zone.

### 3.3. Damping depth in vertically stacked homogeneous profiles ( $d_{shp}$ )

The simulated damping depths from heterogeneous (two layer) profiles ( $d_{2lp}$ ) are compared to damping depths from the vertically stacked homogeneous profiles ( $d_{shp}$ ) (Fig. 6) and used to evaluate the effects of layer interactions and the conditions where the assumption of linear superposition appear most valid. The percent change from  $d_{2lp}$  to  $d_{shp}$  ranges from  $-10\%$  to  $22\%$ , where the negative values indicate that  $d_{2lp} > d_{shp}$  and the positive values indicate that  $d_{2lp} < d_{shp}$  (Fig. 6). The majority of the values are between  $\pm 10\%$  for all three upper-layer thicknesses, and these errors are relatively small compared to the variations of  $d$  within any given period band shown in Fig. 4. Additionally, there is no apparent relationship in the variance of the percent change in  $d$  as a function of upper-layer thickness (Fig. 6). This indicates that  $d_{shp}$  and the assumption of linear superposition are generally not sensitive to the upper-layer thickness for the simulated range of  $q_s$ , monthly to annual P, and for the representative soil textures

of clay, silt, and loam. The profiles of silt over clay and silt over loam resulted in positive value outliers (11–22%) and indicate that  $d_{shp}$  overestimates  $d_{2lp}$  (Fig. 6). Interestingly, the positive outliers occur only for the monthly (30 day) and seasonal (90 day) periods (Fig. 6a and b), and not for the annual (365 day) period (Fig. 6c). The validity of the linear superposition assumption apparently increases as the period increases, and is justification for not showing the error analysis for longer periods, as in Fig. 4.

The results presented in Fig. 6 generally indicate that  $d_{shp}$  is relatively insensitive to the hydraulic interactions between layers and that the assumption of linear superposition may be reasonable for many combinations of soil textures, especially when the soil textures in a layered profile are relatively similar in terms of hydraulic properties and include clay, silt, and loam. The important implications of these findings is that if clay, silt, and loam layers are present in the vadose zone, relatively simple, homogeneous models may provide reasonably accurate estimates of the depth of transient recharge in response to climate variability. A more detailed follow-up paper will examine the phenomena controlling signal propagation across the layer boundaries.

## 4. Summary and conclusions

We use simple numerical modeling experiments to demonstrate that cyclical infiltration in the vadose zone from variable climate could result in variable recharge and potentially impact the availability of groundwater resources. We evaluated hundreds of numerical HYDRUS-1D simulations over a range of periodic boundary conditions and vadose zone geometries and hydraulic parameters that are generally representative of aquifer systems of the conterminous U.S., and likely found throughout the world. The periods of the variations match those of known climate cycles, and the fluxes are representative of arid to humid climates. We focused on simulated damping depth in the vadose zone, which is defined where the ratio of the flux variation at any depth to the infiltration flux variation from the sinusoidal perturbation at land surface is equal to 5%. Understanding the physical processes that control damping depth is central to understanding and predicting climate variability teleconnections with groundwater level variability because the vertical position of the damping depth in the vadose zone determines the presence of steady-state or transient recharge at the water table.

Results of the simulated damping depths provide important insight into the appropriate conditions and limitations of using the assumption of steady-state recharge fluxes for aquifers across the U.S., and how oscillations associated with global-scale climate variability result in transient recharge at local scales. The findings presented here provide a framework that generally explains why some periodic infiltration fluxes associated with climate variability are unexpectedly absent in groundwater level fluctuations and dampen with depth in the vadose zone, resulting in steady-state recharge fluxes, while other periodic surface fluxes do not dampen with depth, resulting in transient recharge.

We find that damping depth spans several orders of magnitude, depending on the mean flux and period of the time varying infiltration that may be associated with global scale climate patterns, as well as the soil texture and hydraulic properties of the local vadose zone. Damping depth generally increases as mean flux and period of the time varying infiltration increase and the vadose zone contains relatively more coarser-soil textures. Given the general differences in climate and depths to water, a wider range of time-varying recharge fluxes, from monthly to decadal-scale variability, are likely to be present at the water table in aquifers of the humid eastern U.S., while a more narrow range of time-varying recharge fluxes, from interannual to decadal timescales are more likely to be present at the water table in aquifers of the

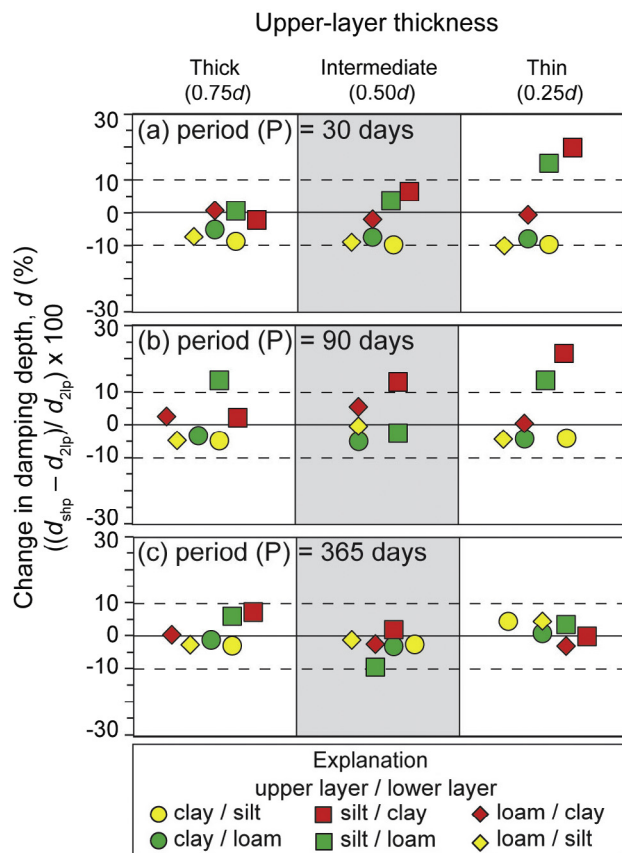


**Fig. 6.** The percent change (%) between 54 HYDRUS-1D simulations of damping depth in heterogeneous (two layer) profiles ( $d_{2lp}$ ) and vertically stacked homogeneous profiles ( $d_{shp}$ ) is shown as a function of upper-layer thickness (thick,  $0.75d$ ; intermediate,  $0.5d$ ; and thin,  $0.25d$ ), using  $q_s$  ( $1.0 \text{ mm d}^{-1}$ ) and periods (a) 30 days, (b) 90 days, and (c) 365 days. The negative % values indicate that  $d_{2lp} > d_{shp}$ , and the positive % values indicate that  $d_{2lp} < d_{shp}$ .

semiarid and arid western U.S. Damping of transient recharge fluxes are more likely in the semiarid and arid aquifers of the U.S. that have relatively greater depths to water. However, local conditions or land-use change that create focused or preferential recharge mechanisms could enable the shorter period time-varying recharge fluxes (monthly to annual) to reach the water table in the semiarid and arid aquifers of the western U.S. An important finding here is that given the general range of conditions representative of the continental U.S., transient recharge fluxes in response to the climate variability patterns of AO, NAO, ENSO, and possibly PDO could be detected at the depth of the water table in most aquifers.

An important implication of our findings is that prioritizing the characterization of average recharge fluxes ( $q_c$ ) and climate variability periodicity (P) over site specific soil types, for example during groundwater model development, may yield more accurate estimates of transient versus steady recharge. Application of these findings from simulations of homogeneous soil textures to real-world groundwater resource management objectives has limitations because we find that heterogeneities and layering can have a substantial impact on damping depth under some conditions. However, when the soil textures in a layered profile are relatively similar, especially if they include clay, silt, and loam, homogeneous simulations that use the soil texture at land surface may be reasonable approximations of the depth of transient recharge fluxes as compared to more complex heterogeneous simulations that parameterize layering of texture in the vadose zone. These findings generally support continued work aimed at collecting soil cores and measuring soil hydraulic properties or inferring them from pedotransfer functions or geophysical methods.

Another important finding is that the assumption of linear superposition is reasonable under a considerable range of conditions that we tested. The model results indicate that the damping depth is not sensitive to layer thickness or hydraulic interactions between many combinations of soil textures, especially when the soil textures in a layered profile are relatively similar and include clay, silt, and loam, and thus support the assumption of linear superposition under those conditions. We conclude that the apparent linear behavior in the damping of climate varying recharge fluxes over a considerable range of clay, silt, and loam textures is further support that simple, homogeneous models of soil textures at land surface can reasonably estimate transient recharge fluxes in more complex, layered vadose zone profiles. A follow-up paper will test and validate this framework using results from spectral analyses of hydrologic time series and field observations from the vadose zone where available.

## Acknowledgments

This research was supported by the National Science Foundation (NSF) Hydrologic Sciences program under the award #EAR-1316553; UNESCO Groundwater Resource Assessment under the Pressures of Humanity and Climate Change (GRAPHIC) program; Groundwater@Global Palaeo climate Signals (G@GPS) program (under awards INQUA TERPRO IFG #1616F; and IGCP #618); and two graduate student scholarships (2014–2015; 2015–2016) from the Achievement Rewards for College Scientists (ARCS) Foundation.

## References

- Bakker, M., Nieber, J.L., 2009. Damping of sinusoidal surface flux fluctuations with soil depth. *Vadose Zone J.* 8, 119–126. <http://dx.doi.org/10.2136/vzj2008.0084>.
- Baram, S., Kurtzman, D., Dahan, O., 2012. Water percolation through a clayey vadose zone. *J. Hydrol.* 424–425, 165–171. <http://dx.doi.org/10.1016/j.jhydrol.2011.12.040>.
- Bayari, C.S., Yildiz, F.E., 2012. Effects of the North Atlantic oscillation and groundwater use on the contraction of Sultansazligi Wetland, Turkey. *Hydrogeol. J.* 20, 369–383. <http://dx.doi.org/10.1007/s10040-011-0809-z>.
- Beebee, R.A., Manga, M., 2004. Variation in the relationship between snowmelt runoff in Oregon and ENSO and PDO. *J. Am. Water Resour. Assoc.* 40, 1011–1024.
- Benjamini, Y., Hochberg, Y., 1995. Controlling the false discovery rate: a practical and powerful approach to multiple testing. *J. R. Stat. Soc. Ser. B.* 289–300.
- Brabets, T.P., Walvoord, M.A., 2009. Trends in streamflow in the Yukon River Basin from 1944 to 2005 and the influence of the Pacific Decadal oscillation. *J. Hydrol.* 371, 108–119. <http://dx.doi.org/10.1016/j.jhydrol.2009.03.018>.
- Carrera-Hernandez, J.J., Mendoza, C.A., Devito, K.J., Petrone, R.M., Smerdon, B.D., 2011. Effects of aspen harvesting on groundwater recharge and water table dynamics in a subhumid climate. *Water Resour. Res.* 47, W05542. <http://dx.doi.org/10.1029/2010WR009684>.
- Cayan, D.R., Redmond, K.T., Riddle, L.G., 1999. ENSO and hydrologic extremes in the Western United States\*. *J. Clim.* 12, 2881–2893.
- Chen, C., Cane, M.A., Wittenberg, A.T., Chen, D., 2017. ENSO in the CMIP5 simulations: life cycles, diversity, and responses to climate change. *J. Clim.* 30, 775–801. <http://dx.doi.org/10.1175/JCLI-D-15-0901.1>.
- Corona, C.R., 2016. Climate variability and vadose zone controls on damping of transient recharge fluxes (MS thesis). San Francisco State University, San Francisco, CA.
- Dickinson, J.E., Ferré, T.P.A., Bakker, M., Crompton, B., 2014. A screening tool for delineating subregions of steady recharge within groundwater models. *Vadose Zone J.* 13, 15. <http://dx.doi.org/10.2136/vzj2013.10.0184>.
- Dickinson, J.E., Hanson, R.T., Ferré, T.P.A., Leake, S.A., 2004. Inferring time-varying recharge from inverse analysis of long-term water levels. *Water Resour. Res.* 40. <http://dx.doi.org/10.1029/2003WR002650>.
- Enfield, D.B., Mestas-Núñez, A.M., Trimble, P.J., 2001. The Atlantic multidecadal oscillation and its relation to rainfall and river flows in the continental U.S. *Geophys. Res. Lett.* 28, 2077–2080.
- Famiglietti, J.S., 2014. The global groundwater crisis. *Nat. Clim. Change* 4, 945–948. <http://dx.doi.org/10.1038/nclimate2425>.
- Fan, Y., Miguez-Macho, G., Weaver, C.P., Walko, R., Robock, A., 2007. Incorporating water table dynamics in climate modeling: 1. Water table observations and equilibrium water table simulations. *J. Geophys. Res.* 112. <http://dx.doi.org/10.1029/2006JD008111>.
- Fleming, S.W., Quilty, E.J., 2006. Aquifer responses to El Niño–Southern oscillation, Southwest British Columbia. *Ground Water* 44, 595–599. <http://dx.doi.org/10.1111/j.1745-6584.2006.00187.x>.
- Gardner, W.R., 1958. Some steady-state solutions of the unsaturated moisture flow equation with application to evaporation from a water table. *Soil Sci.* 85, 228–232.
- Ghil, M., 2002. Natural Climate Variability, in: Encyclopedia of Global Environmental Change, The Earth System: Physical and Chemical Dimensions of Global Environmental Change. Wiley, Chichester; New York, p. 6.
- Green, T.R., Taniguchi, M., Kooi, H., Gurdak, J.J., Allen, D.M., Hiscock, K.M., Treidel, H., Aureli, A., 2011. Beneath the surface of global change: impacts of climate change on groundwater. *J. Hydrol.* 405, 532–560. <http://dx.doi.org/10.1016/j.jhydrol.2011.05.002>.
- Gurdak, J.J., 2017. Groundwater: climate-induced pumping. *Nat. Geosci.* 10. <http://dx.doi.org/10.1038/ngeo2885>.
- Gurdak, J.J., Hanson, R.T., Green, T.R., 2009. Effects of climate variability and change on groundwater resources of the United States (No. Fact Sheet 2009-3074). U.S. Geological Survey, Reston, VA.
- Gurdak, J.J., Hanson, R.T., McMahon, P.B., Bruce, B.W., McCray, J.E., Thyne, G.D., Reedy, R.C., 2007. Climate variability controls on unsaturated water and chemical movement, High Plains aquifer, USA. *Vadose Zone J.* 6, 533. <http://dx.doi.org/10.2136/vzj2006.0087>.
- Hanson, R.T., Dettinger, M.D., Newhouse, M.W., 2006. Relations between climatic variability and hydrologic time series from four alluvial basins across the southwestern United States. *Hydrogeol. J.* 14, 1122–1146. <http://dx.doi.org/10.1007/s10040-006-0067-7>.
- Hanson, R.T., Newhouse, M.W., Dettinger, M.D., 2004. A methodology to assess relations between climatic variability and variations in hydrologic time series in the southwestern United States. *J. Hydrol.* 287, 252–269. <http://dx.doi.org/10.1016/j.jhydrol.2003.10.006>.
- Holman, I.P., Rivas-Casado, M., Bloomfield, J.P., Gurdak, J.J., 2011. Identifying non-stationary groundwater level response to North Atlantic ocean-atmosphere teleconnection patterns using wavelet coherence. *Hydrogeol. J.* 19, 1269–1278. <http://dx.doi.org/10.1007/s10040-011-0755-9>.
- Holman, I.P., Rivas-Casado, M., Howden, N.J.K., Bloomfield, J.P., Williams, A.T., 2009. Linking North Atlantic ocean-atmosphere teleconnection patterns and hydrogeological responses in temperate groundwater systems. *Hydrol. Processes* 23, 3123–3126. <http://dx.doi.org/10.1002/hyp.7466>.
- Hunt, R.J., Prudic, D.E., Walker, J.F., Anderson, M.P., 2008. Importance of unsaturated zone flow for simulating recharge in a humid climate. *Groundwater* 46, 551–560. <http://dx.doi.org/10.1111/j.1745-6584.2007.00427.x>.
- Hurrell, J.W., 1995. Decadal trends in the North Atlantic oscillation: regional temperatures and precipitation. *Science* 269, 676–679. <http://dx.doi.org/10.1126/science.269.5224.676>.
- Kondrashov, D., Feliks, Y., Ghil, M., 2005. Oscillatory modes of extended Nile River records (A.D. 622–1922). *Geophys. Res. Lett.* 32, 4. <http://dx.doi.org/10.1029/2004GL022156>.
- Kuss, A.J.M., Gurdak, J.J., 2014. Groundwater level response in U.S. principal aquifers to ENSO, NAO, PDO, and AMO. *J. Hydrol.* 519, 1939–1952. <http://dx.doi.org/10.1016/j.jhydrol.2014.09.069>.

- Maheu, C., Cazenave, A., Mechoso, C.R., 2003. Water level fluctuations in the Plata Basin (South America) from Topex/Poseidon Satellite Altimetry. *Geophys. Res. Lett.* 30, 4. <http://dx.doi.org/10.1029/2002GL016033>.
- Mantua, N.J., Hare, S.R., 2002. The Pacific decadal oscillation. *J. Oceanogr.* 58, 35–44.
- Mantua, N.J., Hare, S.R., Zhang, Y., Wallace, J.M., Francis, R.C., 1997. A Pacific interdecadal climate oscillation with impacts on salmon production. *Bull. Am. Meteorol. Soc.* 78, 1069–1079.
- Mathias, S.A., Butler, A.P., 2006. Linearized Richards' equation approach to pumping test analysis in compressible aquifers: Richards' equation approach to pumping test analysis. *Water Resour. Res.* 42. <http://dx.doi.org/10.1029/2005WR004680>.
- Mazouz, R., Assani, A.A., Quessy, J., Légaré, G., 2012. Comparison of the interannual variability of spring heavy flood characteristics of tributaries of the St. Lawrence River in Quebec (Canada). *Adv. Water Resour.* 35, 110–120. <http://dx.doi.org/10.1016/j.advwatres.2011.10.006>.
- McCabe, G.J., Palecki, M.A., Betancourt, J.L., 2004. Pacific and Atlantic Ocean influences on multidecadal drought frequency in the United States. *Proc. Natl. Acad. Sci.* 101, 4136–4141. <http://dx.doi.org/10.1073/pnas.0306738101>.
- Meixner, T., Manning, A.H., Stonestrom, D.A., Allen, D.M., Ajami, H., Blasch, K.W., Brookfield, A.E., Castro, C.L., Clark, J.F., Gochis, D.J., Flint, A.L., Neff, K.L., Niraula, R., Rodell, M., Scanlon, B.R., Singha, K., Walvoord, M.A., 2016. Implications of projected climate change for groundwater recharge in the western United States. *J. Hydrol.* 534, 124–138. <http://dx.doi.org/10.1016/j.jhydrol.2015.12.027>.
- Mora, C., Frazier, A.G., Longman, R.J., Dacks, R.S., Walton, M.M., Tong, E.J., Sanchez, J. J., Kaiser, L.R., Stender, Y.O., Anderson, J.M., Ambrosino, C.M., Fernandez-Silva, I., Giuseffi, L.M., Giambelluca, T.W., 2013. The projected timing of climate departure from recent variability. *Nature* 502, 183–187. <http://dx.doi.org/10.1038/nature12540>.
- NOAA, 2015. Climate Monitoring: Teleconnections [WWW Document]. Natl. Clim. Data Cent. <<http://www.ncdc.noaa.gov/teleconnections/>> (accessed 3.15.15).
- Perez-Valdivia, C., Sauchyn, D., Vanstone, J., 2012. Groundwater levels and teleconnection patterns in the Canadian Prairies. *Water Resour. Res.* 48. <http://dx.doi.org/10.1029/2011WR010930>.
- Pool, D.R., Dickinson, J.E., 2007. Ground-water flow model of the Sierra Vista subwatershed and Sonoran portions of the Upper San Pedro Basin, Southeastern Arizona, United States, and Northern Sonora, Mexico (Scientific Investigations Report No. 2006–5228). U. S. Geological Survey, Reston, VA.
- Ropelewski, C.F., Halpert, M.S., 1986. North American precipitation and temperature patterns associated with the El Niño/Southern Oscillation (ENSO). *Mon. Weather Rev.* 114, 2352–2362.
- Russo, T.A., Lall, U., 2017. Depletion and response of deep groundwater to climate-induced pumping variability. *Nat. Geosci.* 10, 105–108. <http://dx.doi.org/10.1038/ngeo2883>.
- Sabziparvar, A.A., Mirmasoudi, S.H., Tabari, H., Nazemosadat, M.J., Maryanaji, Z., 2011. ENSO teleconnection impacts on reference evapotranspiration variability in some warm climates of Iran. *J. Climatol.* 31, 1710–1723. <http://dx.doi.org/10.1002/joc.2187>.
- Sanford, W.E., Selnick, D.L., 2013. Estimation of Evapotranspiration Across the Conterminous United States Using a Regression With Climate and Land-Cover Data. *JAWRA J. Am. Water Resour. Assoc.* 49, 217–230.
- Schaap, M.G., Leij, F.J., van Genuchten, M.T., 2001. ROSETTA: a computer program for estimating soil hydraulic parameters with hierarchical pedotransfer functions. *J. Hydrol.* 251, 163–176.
- Šimůnek, J., van Genuchten, M.T., Šejna, M., 2008. Development and applications of the HYDRUS and STANMOD software packages and related codes. *Vadose Zone J.* 7, 587–600. <http://dx.doi.org/10.2136/vzj2007.0077>.
- Stoner, A.M.K., Hayhoe, K., Wuebbles, D.J., 2009. Assessing general circulation model simulations of atmospheric teleconnection patterns. *J. Clim.* 22, 4348–4372. <http://dx.doi.org/10.1175/2009JCLI2577.1>.
- Strobach, E., Harris, B.D., Dupuis, J.C., Kepic, A.W., 2014. Time-lapse borehole radar for monitoring rainfall infiltration through podsol horizons in a sandy vadose zone. *Water Resour. Res.* 50, 2140–2163. <http://dx.doi.org/10.1002/2013WR014331>.
- Taniguchi, M., Endo, A., Gurdak, J.J., Swarzenski, P., 2017. Water-energy-food Nexus in the Asia-Pacific Region. *J. Hydrol. Reg. Stud.*
- Taylor, R.G., Scanlon, B., Döll, P., Rodell, M., van Beek, R., Wada, Y., Longuevergne, L., Leblanc, M., Famiglietti, J.S., Edmunds, M., Konikow, L., Green, T.R., Chen, J., Taniguchi, M., Bierkens, M.F.P., MacDonald, A., Fan, Y., Maxwell, R.M., Yecheili, Y., Gurdak, J.J., Allen, D.M., Shamsudduha, M., Hiscock, K., Yeh, P.J.-F., Holman, I., Treidel, H., 2012. Ground water and climate change. *Nat. Clim. Change* 3, 322–329. <http://dx.doi.org/10.1038/nclimate1744>.
- Treidel, H., Martin-Bordes, J.L., Gurdak, J.J. (Eds.), 2012. *Climate Change Effects on Groundwater Resources: A Global Synthesis of Findings and Recommendations*. CRC Press, Taylor & Francis Group, London, UK.
- Tremblay, L., Larocque, M., Anctil, F., Rivard, C., 2011. Teleconnections and interannual variability in Canadian groundwater levels. *J. Hydrol.* 410, 178–188. <http://dx.doi.org/10.1016/j.jhydrol.2011.09.013>.
- Turkeltaub, T., Dahan, O., Kurtzman, D., 2014. Investigation of groundwater recharge under agricultural fields using transient deep vadose zone data 13 (4). doi:10.2136/vzj2013.10.0176.
- Velasco, E.M., Gurdak, J.J., Dickinson, J.E., Ferré, T.P.A., Corona, C.R., 2015. Interannual to multidecadal climate forcings on groundwater resources of the U.S. West Coast. *J. Hydrol. Reg. Stud.* <http://dx.doi.org/10.1016/j.ejrh.2015.11.018>.
- Venencio, M.del V., García, N.O., 2011. Interannual variability and predictability of water table levels at Santa Fe Province (Argentina) within the climatic change context. *J. Hydrol.* 409, 62–70. <http://dx.doi.org/10.1016/j.jhydrol.2011.07.039>.
- Vicente-Serrano, S.M., López-Moreno, J.L., Gimeno, L., Nieto, R., Morán-Tejeda, E., Lorenzo-Lacruz, J., Beguería, S., Azorin-Molina, C., 2011. A multiscale global evaluation of the impact of ENSO on droughts. *J. Geophys. Res.* 116. <http://dx.doi.org/10.1029/2011JD016039>.
- Wolter, K., Timlin, M.S., 2011. El Niño/southern Oscillation behaviour since 1871 as diagnosed in an extended multivariate ENSO index (MEIext). *Int. J. Climatol.* 31, 1074–1087.
- Wraith, J.M., Or, D., 1998. Nonlinear parameter estimation using spreadsheet software. *J. Nat. Resour. Life Sci. Educ.* 27, 13–29.
- Zhang, L., Delworth, T.L., 2016. Simulated response of the Pacific decadal oscillation to climate change. *J. Clim.* 5999–6018. <http://dx.doi.org/10.1175/JCLI-D-15-0690.1>.